JOURNAL OF AGRICULTURAL AND FOOD CHEMISTRY

Article

pubs.acs.org/JAFC

Hispolon Induces Apoptosis through JNK1/2-Mediated Activation of a Caspase-8, -9, and -3-Dependent Pathway in Acute Myeloid Leukemia (AML) Cells and Inhibits AML Xenograft Tumor Growth in Vivo

Pei-Ching Hsiao,[†,∥] Yi-Hsien Hsieh,[†,‡] Jyh-Ming Chow,[#] Shun-Fa Yang,[§,⊥] Michael Hsiao,[▽] Kuo-Tai Hua,[○] Chien-Huang Lin,[◆] Hui-Yu Chen,[§] and Ming-Hsien Chien*[,¶,&]

[†]School of Medicine, [‡]Institute of Biochemistry and Biotechnology, and [§]Institute of Medicine, Chung Shan Medical University, No. 110, Section 1, Chien-Kuo N Road, Taichung 40201, Taiwan

[∥]Department of Internal Medicine, and [⊥]Department of Medical Research, Chung Shan Medical University Hospital, Number 110, Section 1, Chien-Kuo N Road, Taichung 40201, Taiwan

[#]The Section of Hematology-Oncology, Department of Internal Medicine, Wan Fang Hospital, Taipei Medical University, 111, Section 3, Hsing-Long Road, Taipei 116, Taiwan

[▽]Genomics Research Center, Academia Sinica,128 Academia Road, Section 2, Taipei 115, Taiwan

[○]Graduate Institute of Toxicology, College of Medicine, National Taiwan University, 5F Number 1, Section 1, Jen-Ai Road, Taipei 100, Taiwan

[◆]Graduate Institutes of Medical Sciences and [¶]Clinical Medicine, College of Medicine, Taipei Medical University, 250 Wu-Hsing Street, Taipei 110, Taiwan

[&]Wan Fang Hospital, Taipei Medical University, 111, Section 3, Hsing-Long Road, Taipei 116, Taiwan

Supporting Information

ABSTRACT: Hispolon is an active phenolic compound of *Phellinus igniarius*, a mushroom that was recently shown to have antioxidant and anticancer activities in various solid tumors. Here, the molecular mechanisms by which hispolon exerts anticancer effects in acute myeloid leukemia (AML) cells was investigated. The results showed that hispolon suppressed cell proliferation in the various AML cell lines. Furthermore, hispolon effectively induced apoptosis of HL-60 AML cells through caspases-8, -9, and -3 activations and PARP cleavage. Moreover, treatment of HL-60 cells with hispolon induced sustained activation of JNK1/2, and inhibition of JNK by JNK1/2 inhibitor or JNK1/2-specific siRNA significantly abolished the hispolon-induced activation of the caspase-8/-9/-3. In vivo, hispolon significantly reduced tumor growth in mice with HL-60 tumor xenografts. In hispolon-treated tumors, activation of caspase-3 and a decrease in Ki67-positive cells were observed. Our results indicated that hispolon may have the potential to serve as a therapeutic tool to treat AML.

KEYWORDS: *hispolon, apoptosis, acute myeloid leukemia, JNK1/2, caspase, xenograft tumor*

INTRODUCTION

Acute myeloid leukemia (AML) is an aggressive malignancy characterized by rapid growth of abnormal white blood cells (WBCs). AML is primarily treated by chemotherapy, and radiotherapy is rarely applied.[1] Although conventional chemotherapy of AML with either cytarabine or daunorubicin given as a single agent induces complete remission in ∼30−40% of patients and combination treatment with both agents induces complete remission in more than 50% of patients,[2] only 20−30% of patients enjoy long-term disease-free survival[2] and these chemo drugs can also affect normal cells causing unpleasant side effects such as anemia, bleeding, and infection. Thus, there is a need for new agents to treat AML.

In recent years, some natural products have been used as alternative treatments for cancers including AML because of their extensive biological activities and comparatively low toxicities. For instance, wogonin, an active compound in *Scutellaria baicalensis*, induces apoptosis by inhibiting telomerase activity in HL-60 AML cells,[3] and icariside II, a flavonoid compound derived from *Epimedium koreanum*, was suggested as an antileukemic agent for AML therapy.[4] Moreover, matrine, an alkaloid extracted from *Sophora flavescens* Aif, targets mitochondrial apoptotic pathways in HL-60 and primary AML cells.[5]

Phellinus linteus (PL), a traditional medicinal mushroom, is commonly called "Sanghwang" in Taiwan. It is popular in Oriental countries such as China, Korea, and Japan. PL contains many bioactive compounds and is known to improve health and prevent and remedy various diseases, such as gastroenteric disorders, lymphatic diseases, and cancer.[6] A few pharmacological actions of PL were recently elucidated. For instance, PL

Received: July 5, 2013
Revised: September 30, 2013
Accepted: October 4, 2013
Published: October 4, 2013

dx.doi.org/10.1021/jf402956m | J. Agric. Food Chem. 2013, 61, 10063−10073

suppresses cellular proliferation and induces apoptosis in lung and prostate cancer cells.[7,8] The antimetastatic effects of PL were demonstrated against in vivo colon cancer and melanoma models.[9,10] PL was also found to inhibit the growth, angiogenesis, and invasive behavior of breast cancer cells via suppressing AKT phosphorylation.[11] Hispolon, a phenol compound isolated from PL, possesses anti-inflammatory, antiproliferative, and antioxidant effects[12,13] and exerts protective effects on acute liver damage[14] and balloon-injured neointimal formation.[15] Additionally, accumulating evidence indicates that hispolon also possesses an antitumor effect by inhibiting tumor cell growth or metastasis in various solid tumor types.[16−20] However, there are no reports concerning the anticancer effects of hispolon on nonsolid tumors. In the present study, we investigated the cytotoxic effects of hispolon on AML cell lines, THP-1, U937, HL-60, OCI, MV4-11, and MOLM-13 and its underlying mechanisms in vitro and in vivo.

MATERIALS AND METHODS

Materials. Hispolon of 98% purity was purchased from Santa Cruz Biotechnology (Santa Cruz, CA). A 20 mM stock solution of hispolon was made in dimethyl sulfoxide (DMSO) (Sigma, St. Louis, MO) and stored at −20 °C. The final concentration of DMSO for all treatments was <0.5%. Antibodies, specifically of Bax, Bcl-2, cleaved caspase-3, caspase-8, caspase-9, poly(ADP-ribose) polymerase (PARP), p-extracellularly regulated kinase (ERK)1/2, p-p38, p-c-Jun N-terminal kinase (JNK), ERK1/2, p38, JNK1/2, and β-actin (for the Western blot analysis), were purchased from Santa Cruz Biotechnology. An antibody specific for Ki67 (for immunohistochemical staining) was purchased from DAKO (Hamburg, Germany). 4′,6-Diamidino-2-phenylindole (DAPI) was purchased from Sigma. The p38 mitogen-activated protein kinase (MAPK) inhibitor, SB202190, ERK1/2 inhibitor, U0126, and JNK1/2 inhibitor, and SP600125 were purchased from Calbiochem (San Diego, CA). Unless otherwise specified, other chemicals used in this study were purchased from Sigma.

Cell Culture. Human AML cell lines of OCI-AML3, MOLM-13, and MV4-11 were kindly provided by Dr. L.-I. Lin (National Taiwan University, Taipei, Taiwan), while the HL-60, U937, and THP-1 cell lines were purchased from the American Type Culture Collection (ATCC) (Manassas, VA). Human normal cells of WI-38 (lung fibroblast), hTERT-HPNE (pancreas duct epithelium cell), and PNT2 (prostate epithelium cell) were purchased from ATCC or Sigma. All cells were cultured in the recommended conditions, supplemented with 10% heat-inactivated fetal bovine serum (FBS; Gibco, Grand island, NY), 0.1 mM nonessential amino acids, 2 mM L-glutamine, 100 U/mL penicillin, and 100 μg/mL streptomycin.

In Vitro Cytotoxicity Assay. AML cells (OCI-AML3, MOLM-13, MV4-11, HL-60, U937, and THP-1) or normal cells (WI-38, PNT2, and hTERT-HPNE) were plated in 96-well microtiter plates and treated with various concentrations of hispolon for 48 h, and cell viabilities were assessed using an MTS (Promega, Madison, WI) assay. Absorbance (A) was read at 490 nm using an enzyme-linked immunosorbent assay (ELISA) reader (MQX200; Bio-Tek Instruments, Winooski, VT). The cell viability rate (multiples) was determined by $A_{490,\text{hispolon}}/A_{490,\text{vehicle}}$.

Cell Proliferation Assay. Proliferation of AML cells was measured by direct cell counting using a hemocytometer. Briefly, cells were seeded at a density of 1×10^5 cells/well in a 12-well culture plate, grown in RPMI containing 10% FBS, and then treated with 0.5% DMSO without (control) or with various concentrations of hispolon. Medium without or with hispolon was changed daily until cell counting.

Flow Cytometric Analysis. HL-60 cells (2×10^6/mL) were treated with vehicle (0.5% DMSO) or hispolon at various concentrations, and the mixture was allowed to incubate for 24 h (concentration-dependent study) or various time points (time-dependent study). At the end of incubation, cells were collected and fixed with 70% ethanol. Cells were stained with propidium iodide (PI) buffer (4 μg/mL PI, 1% Triton X-100, and 0.5 mg/mL RNase A in phosphate-buffered saline (PBS)) for 30 min in the dark at room temperature and then filtered through a 40 μm nylon filter (Falcon, San Jose, CA). The cell cycle distribution was analyzed for 10 000 collected cells by a FACS Vantage flow cytometer that uses the Cellquest acquisition and analysis program (Becton-Dickinson FACS Calibur, San Jose, CA). Apoptotic cells with hypodiploid DNA content were detected in the sub-G_1 region. All results were obtained from three independent experiments.

Annexin-V/PI Staining Assay. Apoptosis-mediated cell death of tumor cells was examined using a double-staining method with an FITC-labeled Annexin-V/PI Apoptosis Detection kit (BD Biosciences, San Jose, CA). For PI and Annexin-V double staining, cells were suspended in 100 μL of binding buffer (10 mM HEPES/NaOH, 140 mM NaCl, and 2.5 mM $CaCl_2$ at pH 7.4) and stained with 5 μL of FITC-conjugated Annexin-V and 5 μL of PI (50 μg/mL) for 30 min at room temperature in the dark, and then 400 μL of binding buffer was added. Apoptotic cells were analyzed via flow cytometry by a FACScan system flow cytometric analysis. Data acquisition and analysis were performed in a Becton-Dickinson FACS Calibur flow cytometer using Cell Quest software.

DAPI Staining. HL-60 cells were treated with 50 μM hispolon for 24 h and seeded on a slide via cytospinning. Apoptotic morphological changes were assessed via DAPI staining, as previously described.[21]

Mitochondrial Membrane Potential Measurement. Breakdown of mitochondrial membrane potential was determined by FACS analyses using JC-1 (5,5′,6,6′-tetrachloro-1,1′,3,3′-tetraethylbenzimidazolcarbocyanine iodide), which allows one to detect changes in the mitochondrial membrane potential. For this purpose the Mitochondrial Membrane Potential Detection Kit (Immunochemistry, Bloomington, MN) was used, as described in the manufacturer's instruction. There were 10^6 HL60 cells treated for 24 h with the tested drugs. After PBS washing, cells were incubated for 10 min in freshly prepared JC-1 solution (10 μg/mL in culture medium) at 37 °C. Spare dye was removed by PBS washing, and cell-associated fluorescence was measured with FACS.

Small Interfering (si) RNA Transfection. HL-60 cells were transiently transfected with JNK-siRNA or control-siRNA (40 nM) (Santa Cruz Biotechnology) for 8 h using the INTERFERinTM transfection reagent (Polyplus-Transfection, New York, NY) according to the manufacturer's protocols.

Western Blot Analysis. Cell lysates were prepared as previously described.[22] Equal amounts of protein extracts (20 μg) were subjected to 10% or 12% sodium dodecylsulfate polyacrylamide gel electrophoresis (SDS-PAGE) and blotted onto a polyvinylidene fluoride membrane (Millipore, Belford, MA). After blocking, the membrane was incubated with primary antibodies for caspases-9, -3, and -8, PARP, ERK1/2, p-ERK1/2, p38, JNK1/2, p-JNK1/2, Bax, Bcl-2, and β-actin. Blots were then incubated with a horseradish peroxidase-conjugated antimouse or antirabbit antibody. Signals were detected via enhanced chemiluminescence using Immobilon Western HRP Substrate (Millipore, Billerica, MA).

Animals. Age-matched NOD/SCID-IL2Rγ^{null} (NSG) male mice (6−8 weeks old) were used as tumor xenograft models. All animals were maintained in cages in a specifically designed pathogen-free isolation facility with a 12/12 h light/dark cycle. Mice were provided with rodent chow and water ad libitum. All experiments were conducted in accordance with guidelines of the Taipei Medical University Animal Ethics Research Board.

In Vivo Antileukemic Effects on Xenograft Transplantation. HL-60 cells (2×10^6) in 0.1 mL of RPMI 1640 were subcutaneously injected into the right flank of NSG mice. After transplantation, tumor size was measured using calipers and the tumor volume was estimated by the following formula: tumor volume (mm^3) = length × width^2 × 1/2. Once the tumor reached a volume of 250 mm^3, animals began receiving intraperitoneal (i.p.) injections of DMSO or hispolon (5 and 10 mg/kg) in DMSO 5 times per week for 2 weeks. Each mouse was weighed every 2 days to evaluate the side effects of administration, and the tumor size was measured. Mice were sacrificed at 15 days after the

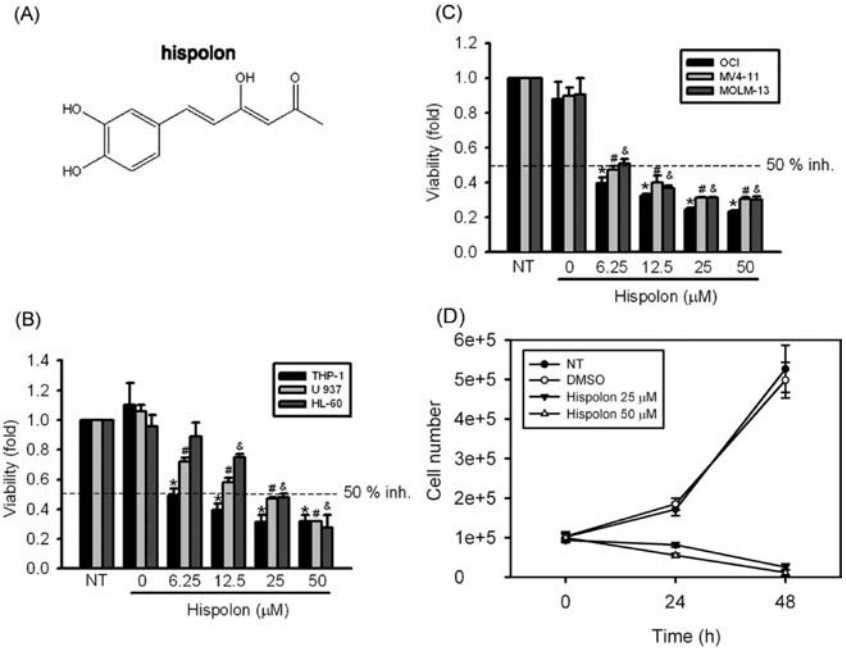

Figure 1. Effect of hispolon on the cell viability of AML cell lines. (A) Chemical structure of hispolon. (B and C) Six AML cell lines were treated with the vehicle (DMSO) or hispolon (6.25−50 μM) in serum-containing medium for 48 h. Cell viability was determined by an MTS assay. Results are expressed as multiples of cell viability. Values represent the mean ± SE of 3 independent experiments. ($^{*, \#, \&}$) $p < 0.05$ compared to the vehicle groups. (D) HL-60 cells were treated with 25 or 50 μM of hispolon for 24 and 48 h and analyzed by trypan blue exclusion assay. Quantitative assessment of the mean number of cells is expressed as means ± SE.

hispolon or DMSO injections. Tumor masses were then excised for immunohistochemical staining and Western blot analysis.

Immunohistochemistry. Tumor tissues were paraffin embedded, sectioned, and processed for immunohistochemical staining as previously described.[23] Staining was detected using the streptavidin−biotin peroxidase complex method with the DAB Peroxidase Substrate Kit (SK-4100; Vector Laboratories) and counterstained with hematoxylin (Merck, Darmstadt, Germany). A proliferation index was determined by Ki67 immunostaining, and Ki67-positive cells were counted in four 400× fields per HL-60 tumor section.

Statistical Analysis. Values are shown as the mean ± SE. Statistical analyses were performed using the Statistical Package for Social Science software, version 16 (SPSS, Chicago, IL). Data comparisons were performed with Student's t test when two groups were compared. A one-way analysis of variance (ANOVA) followed by Tukey's posthoc test was used when more than three groups were analyzed. Differences were considered significant at the 95% confidence level when $p < 0.05$.

RESULTS

Effect of Hispolon on the Cell Viability of AML Cell Lines. The chemical structure of hispolon is shown in Figure 1A. To determine the efficacy of hispolon in vitro in AML cells, we first treated AML cell lines with hispolon. The cytotoxic effects of hispolon were examined in six AML cell lines which represent different French−American−British (FAB) types (M2: HL-60; M4: OCI-AML3; and M5: MOLM-13, MV4-11, U937, and THP-1) and three normal cells (WI-38, PNT2, and hTERT-HPNE). As shown in Figure 1B and 1C, after treatment for 48 h, hispolon significantly reduced the cell viability in a concentration-dependent manner and the 50% growth inhibition concentration (IC_{50}) values were around 6.25−25 μM for the six AML cell lines. Moreover, the IC_{50} values in three human normal cells ($IC_{50} > 100$ μM) (Figure 1, Supporting Information) were higher than AML cell lines after treatment with hispolon for 48 h. We further studied the antiproliferation activity of hispolon on AML cells using cell counting. As illustrated in Figure 1D, hispolon time and concentration dependently decreased the number of cultured HL-60 cells. These results indicated that hispolon can potently inhibit proliferation of different AML FAB types.

Hispolon Induces HL-60 Cells Apoptosis. Physiological cell death is characterized by apoptotic morphology, including chromatin condensation, membrane blebbing, internucleosomal degradation of DNA, and apoptotic body formation. To investigate the mode of cell death induced by hispolon, HL-60 cells were treated with different concentrations (0−50 μM) of hispolon for 24 h or 50 μM hispolon for different time points (0−48 h). It was shown that hispolon induced concentration-dependent decreases in the Bcl-2/Bax ratio (Figure 2A) and increases of the sub-G_1 population (Figure 2B). Moreover, hispolon also induced time-dependent increases in the sub-G_1 population (Figure 2C). Similarly, as shown in Figure 2D, we assessed the translocation of phosphatidylserine (PS) using Annexin-V and PI double staining. Early apoptotic cells (Annexin-V positive) increased from 8.72% to 40.07% and 71.72% after treating HL-60 cells with 25 and 50 μM hispolon, respectively. Moreover, the effect of hispolon on cell morphology was examined using fluorescence microscopy. Cells treated with 50 μM hispolon for 24 h demonstrated morphology characteristic of apoptosis, such as chromatin condensation and formation of apoptotic bodies (Figure 2E, arrows). These results are all hallmarks of apoptotic cell death and demonstrated the ability of hispolon to induce apoptosis in HL-60 cells.

Hispolon Induces Caspase Activation and Loss of Mitochondrial Membrane Potential in HL-60 Cells. The apoptotic process is executed by a member of the highly conserved caspases, and modulation of the mechanisms of caspase activation and suppression is a critical molecular target

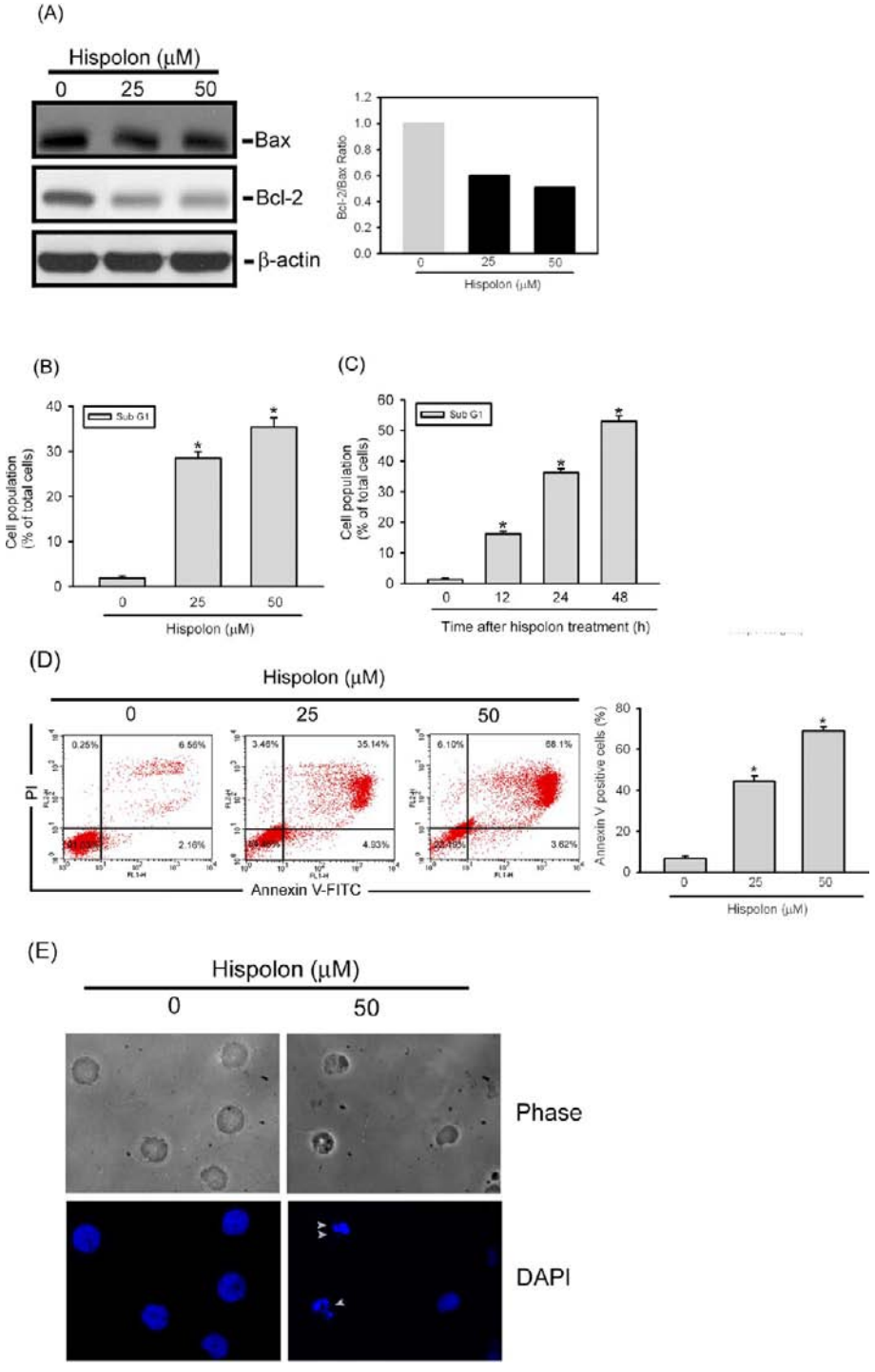

Figure 2. Effect of hispolon on HL-60 cell apoptosis. (A) HL-60 cells were treated with different concentration sof hispolon (0−50 μM) for 24 h and analyzed by Western blotting to detect the Bcl-2/Bax ratio. (B and C) HL-60 cells were treated with different concentrations of hispolon (0−50 μM) for 24 h (B) or 50 μM hispolon for different time points (0−48 h) (C) and analyzed by flow cytometry to detect the cell death in the sub-G_1 phase. (D) Quantitative analysis of cell apoptosis by Annexin-V and PI double-staining flow cytometry. Values represent the mean ± SE of three independent experiments. (*) $p < 0.05$, compared to the vehicle group. (E) HL-60 cells were treated with 50 μM hispolon for 24 h and analyzed by fluorescence microscopy after DAPI staining. White arrows indicate apoptotic HL-60 cells.

in chemoprevention, since these processes lead to apoptosis.[24] To identify the mechanisms underlying hispolon-induced apoptosis in HL-60 cells, activation of caspases-8, -9, and -3 and cleavage of PARP were detected. Figure 3A shows that exposure of HL-60 cells to hispolon (0−50 μM for 24 h) caused concentration-dependent degradation of procaspases-8, -9, and -3, which generated fragments of caspases-8, -9, and -3. Hispolon treatment at 12.5, 25, and 50 μM for 24 h significantly increased expression levels of cleaved PARP by 2.62-, 5.23-, and 22.9-fold, respectively, compared to the control (Figure 3B). Moreover, treatment of HL-60 cells with hispolon (50 μM) also resulted in a time-dependent increase in activated caspases-8, -9, and -3 with a maximal effect at 8−12 or 12−24 h (Figure 3C). The results indicate that hispolon may

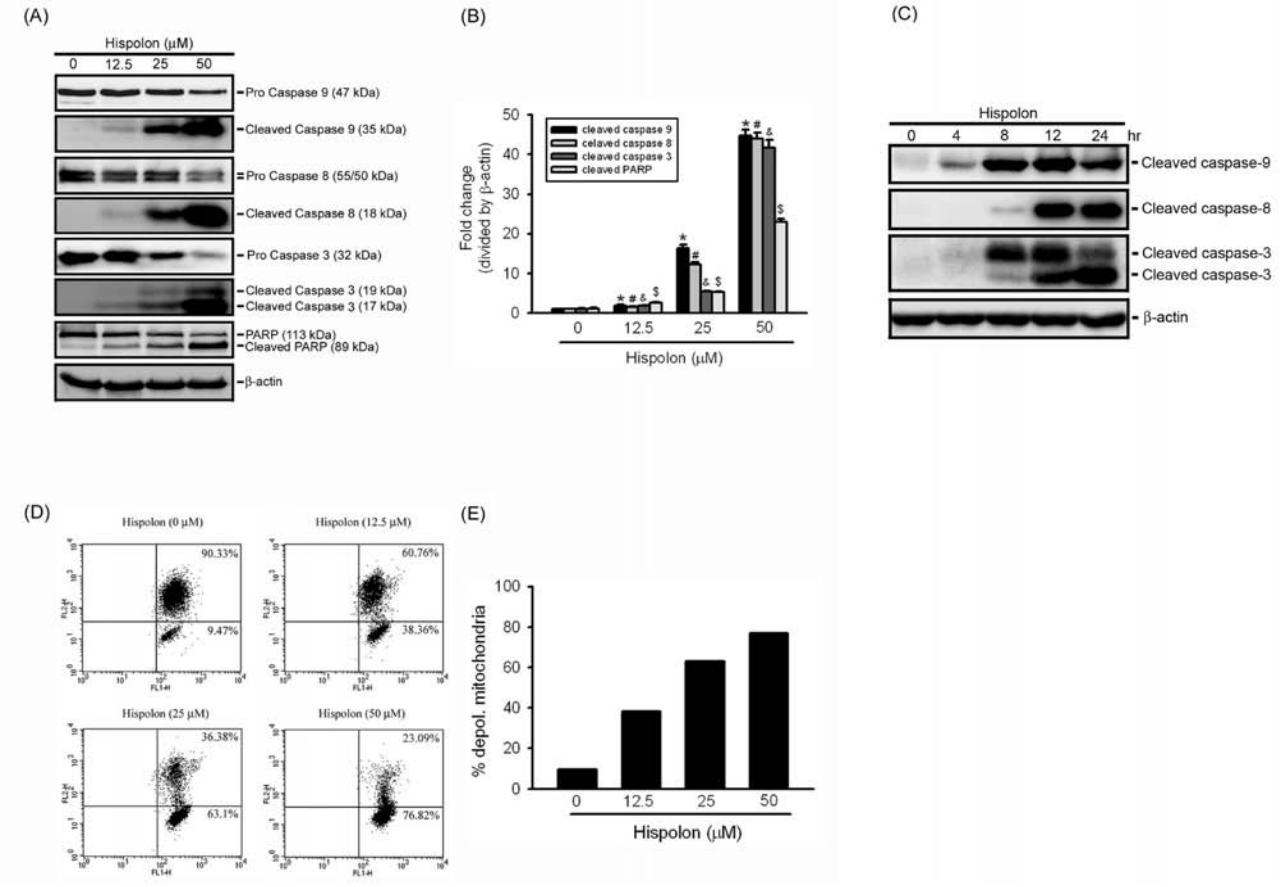

Figure 3. Hispolon induces caspase activation and loss of mitochondrial membrane potential in HL-60 cells. (A) Expression levels of caspase-3, -8, and -9, and PARP were assessed by Western blot analysis after treatment with various concentrations of hispolon (0−50 μM) for 24 h. (B) Quantitative results of cleaved caspase-3, -8, and -9 and PARP protein levels, which were adjusted to the β-actin protein level and expressed as multiples of induction beyond each respective control. Values represent the mean ± SE of three independent experiments. ($^{*, \#, \&, \$}$) $p < 0.05$ compared to the vehicle control groups. (C) Activated caspase-9, -8, and -3 protein expression were upregulated in a time-dependent fashion after hispolon (50 μM) treatment, peaking at 8−12 or 12−24 h in HL-60 cells. (D) Loss of mitochondrial membrane potential after 24 h treatment with hispolon was determined by JC-1 staining. Increases of the green fluorescent apoptotic (FL 1) populations of HL-60 at the indicated drug concentrations (cells in the lower right field) are indicated. (E) Percentages of HL-60 cells with depolarized mitochondria (JC-1 staining) after treatment with different concentrations of hispolon were determined after 24 h treatment.

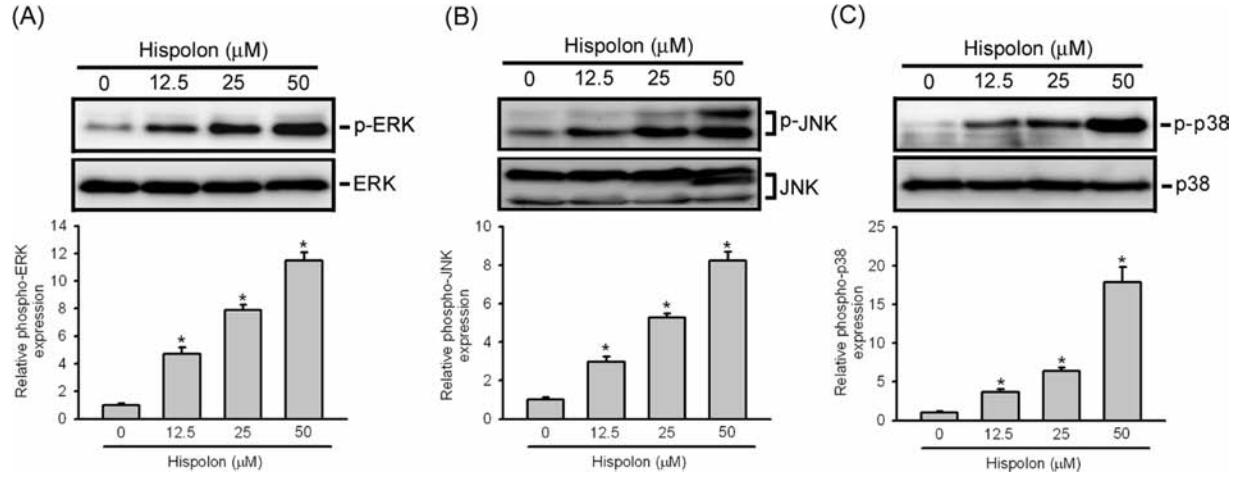

Figure 4. Effect of hispolon on the MAPK pathway. (A−C, upper panel) Phosphorylation levels of ERK1/2, p38, and JNK1/2 were assessed by Western blot analysis after treatment with various concentrations of hispolon (0−50 μM) for 24 h. (A−C, lower panel) Quantitative results of phopho-ERK1/2, p38, and JNK1/2 protein levels, which were adjusted with the total ERK1/2, p38, and JNK1/2 protein levels and expressed as multiples of induction beyond each respective control. Values represent the mean ± SE of three independent experiments. (*) $p < 0.05$ compared to the vehicle control group.

dx.doi.org/10.1021/jf402956m | J. Agric. Food Chem. 2013, 61, 10063−10073

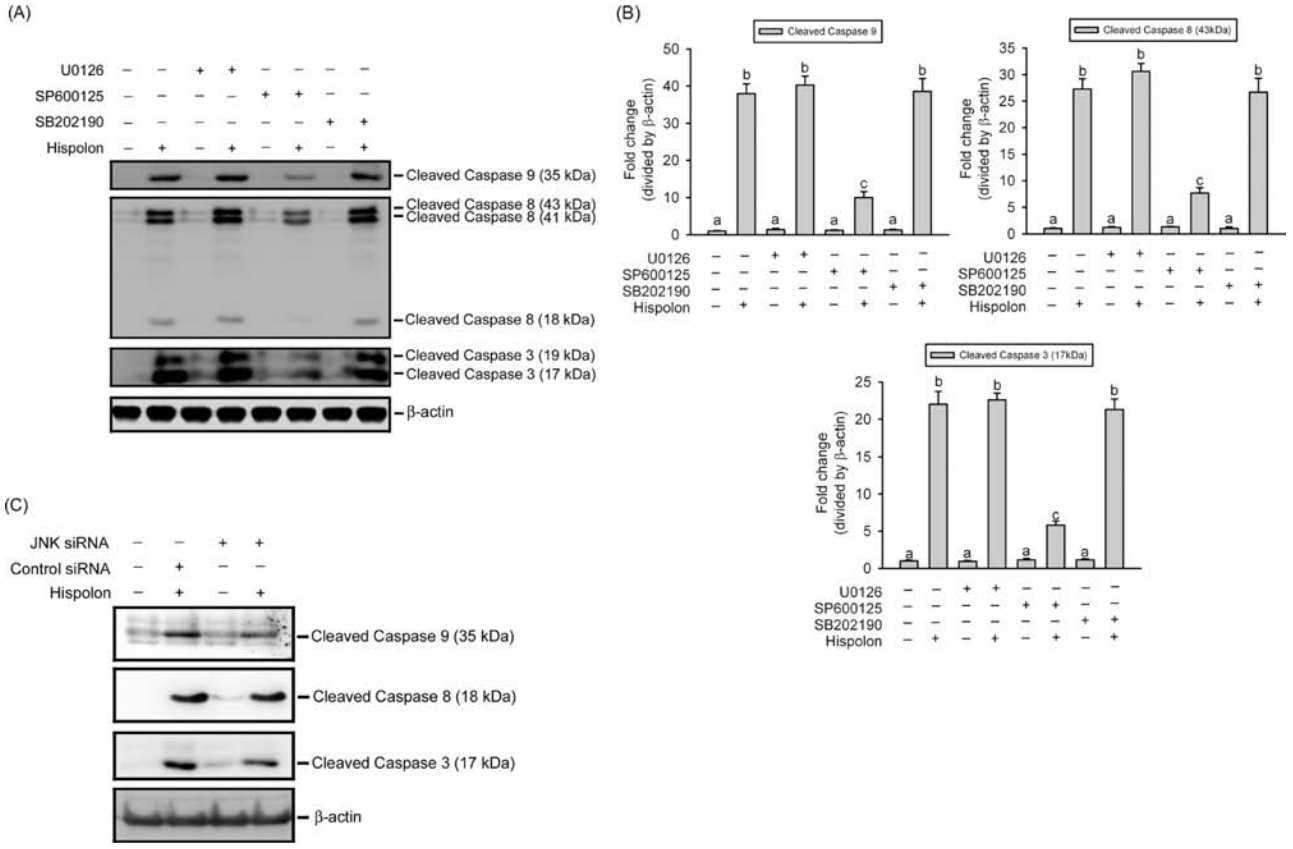

Figure 5. JNK1/2 is essential for caspase activation induced by hispolon. (A) HL-60 cells were pretreated with or without 20 μM U0126, SP600125, or SB202190 for 1 h followed by hispolon (25 μM) treatment for an additional 24 h. Expression levels of cleaved caspase-3, -8, and -9 were determined by Western blot analysis. (B) Quantitative results of cleaved caspase-3, -8, and -9 protein levels, which were adjusted to the β-actin protein level and expressed as multiples of induction beyond each respective control. Values represent the mean ± SE of three independent experiments. Data were analyzed using a one-way ANOVA with Tukey's posthoc tests at 95% confidence intervals; different letters represent different levels of significance. (C) JNK-specific siRNA but not control siRNA partially blocked the hispolon-induced activation of caspase-3, -8, and -9. HL-60 cells were transfected with siRNAs for 8 h followed by hispolon (25 μM) treatment for an additional 24 h prior protein extraction.

have acted through the initiator caspase-8 or -9 and then the executioner caspase-3 to increase the cleavage form of PARP.

To further detect whether hispolon-induced apoptotic cell death is executed by involving the mitochondrial pathway, the fluorescent cationic dye, JC-1, was used to detect the mitochondrial permeability transition. Collapse of the mitochondrial membrane potential is an early step in the induction of apoptosis by the intrinsic pathway.[25] In healthy, non-apoptotic cells the dye accumulates and aggregates within the mitochondria, resulting in bright red staining. In apoptotic cells, due to collapse of the membrane potential, JC-1 cannot accumulate within the mitochondria and remains in the cytoplasm in its green-fluorescent monomeric form. In Figure 3D and 3E, FACS analyses of JC-1-stained HL60 cells treated with hispolon for 24 h are shown. Hispolon induced concentration-dependent collapse of mitochondrial membrane potential, and 50 μM hispolon led to mitochondrial damage in nearly 80% of HL-60 cells.

Involvement of JNK1/2 in Hispolon-induced Activation of Caspases-8, -9, and -3. Studies showed that the MAPK signaling pathway plays an important role in the action of chemotherapeutic drugs.[26] Therefore, we determined whether MAPKs were activated in hispolon-treated HL-60 cells by a Western blot analysis using specific antibodies against the phosphorylated (activated) forms of the kinases. Surprisingly, hispolon induced activation of all MAPKs including ERK1/2, JNK1/2, and p38 in dose-dependent manners (Figure 4). Next, we further investigated relationships among hispolon-induced activation of caspases-8, -9, and -3 and MAPKs. HL-60 cells were pretreated with 20 μM U0126 (an ERK inhibitor), SP600125 (a JNK inhibitor), or SB202190 (a p38 inhibitor) for 1 h, treated with 25 μM hispolon for another 24 h, and then analyzed by Western blotting. As shown in Figure 5, only SP600125 significantly attenuated hispolon-induced caspase-8, -9, and -3 activation (Figure 5A and 5B). Moreover, we also found that JNK activation occurred at earlier time than caspases-8, -9, and -3 activation after hispolon treatment (Figures 3C and S2, Supporting Information). These findings suggest that activation of JNK1/2 might play a critical upstream role in hispolon-mediated caspase activation in HL-60 cells. To further demonstrate that hispolon-induced activation of JNK1/2 in HL-60 cells was correlated with caspase activation, we transiently transfected HL-60 cells with JNK siRNA and examined its effects on hispolon-induced caspase signaling events. Blockage of JNK1/2 by siRNA significantly prevented hispolon-induced activation of caspases-8, -9, and -3 (Figure 5C). These data indicated that hispolon-induced cell apoptosis was dependent on JNK1/2 activation and the subsequent caspase-8/-9/-3 pathway.

Hispolon Suppresses Tumor Cell Proliferation in HL-60 Xenograft Mice. Following the investigation of hispolon-induced cell apoptosis in AML in vitro, the in vivo antitumor

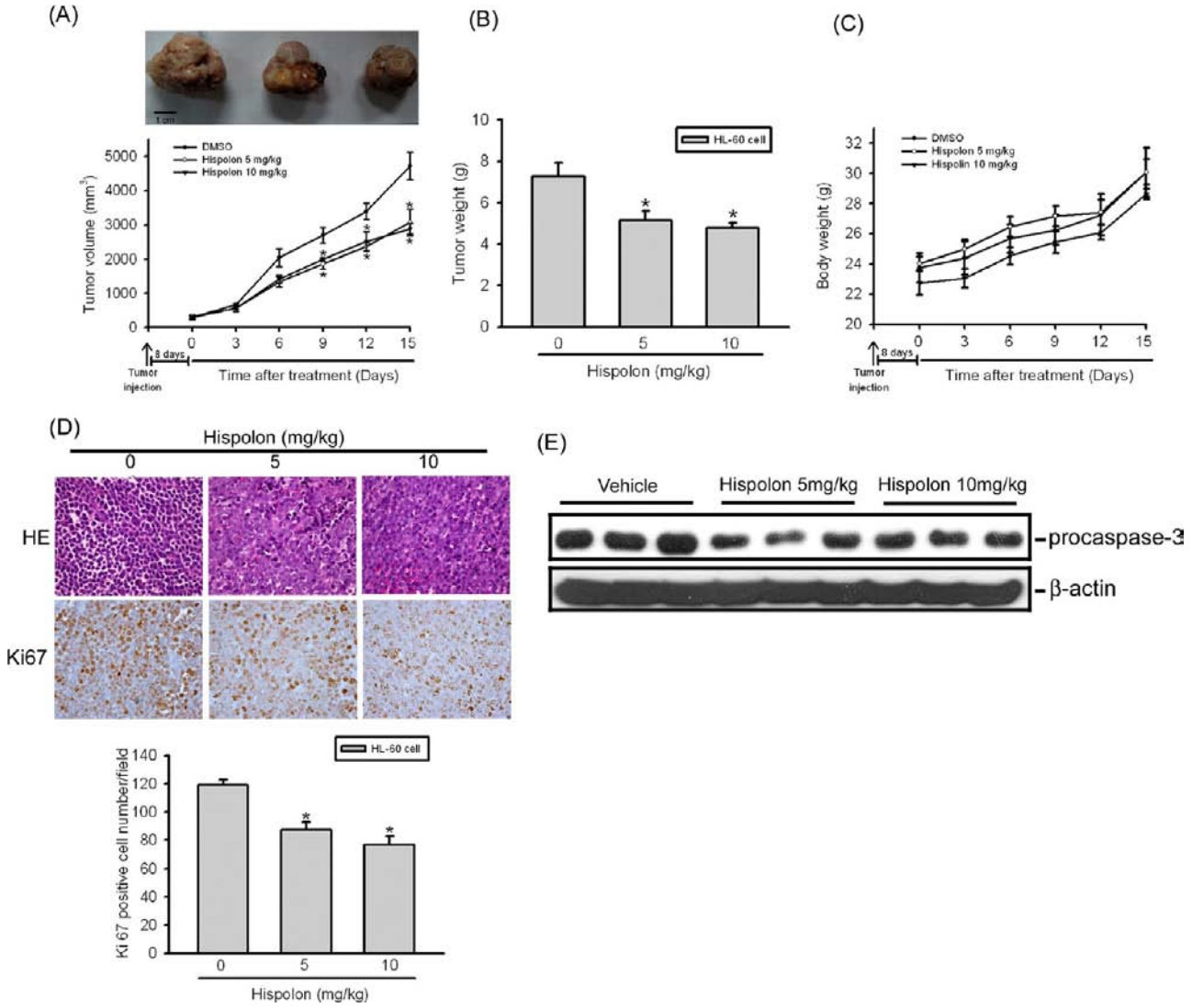

Figure 6. Inhibitory effects of hispolon on tumor growth in vivo. (A) Hispolon reduced the growth rate of tumors in NOD/SCID IL2Rg^{null} (NSG) mice. (Upper panel) Gross appearance of subcutaneous tumors after treatment with DMSO or hispolon for 15 days. Scale bar, 1 cm. (Lower panel) Average tumor volume of DMSO-treated (filled circle, $n = 6$) vs hispolon-treated ((open circle) 5 mg/kg, $n = 6$; (filled triangle) 10 mg/kg, $n = 6$) NSG mice. Intraperitoneal injections of hispolon were initiated when tumors had reached an average size of 250 mm^3. Hispolon treatment reduced tumor weights (B) but did not affect body weights (C). Tumor weights were compared between hispolon-treated and vehicle-treated tumor-bearing mice at the end of the study. Values represent the mean ± SE ($n = 6$). (*) $p < 0.05$ compared to the vehicle-treated group. (D) Hispolon-induced inhibition of proliferation in HL-60-xenografted tumors. A proliferation index was determined by Ki67 immunostaining, and Ki67-positive cells were counted in four 400× fields per HL-60 tumor section. H&E-stained sections showed the histologic morphology. Values represent the mean ± SE ($n = 6$). (*) $p < 0.05$ compared to the vehicle-treated group. (E) Hispolon induced caspase-3 activation in HL-60-xenografted tumors. HL-60 tumors were isolated for protein extraction at 15 days after DMSO or hispolon treatment. Membranes were also probed with an anti-β-actin antibody to verify equivalent protein loading.

effect of hispolon was evaluated. We established a xenograft tumor-bearing model by transplanting HL-60 cancer cells into NSG mice. Dosing with hispolon was begun 8 days after implantation, when the tumors had reached ~250 mm^3. HL-60 xenograft mice were treated with hispolon (5 and 10 mg/kg, i.p.) or the vehicle (control) 5 times per week for 2 weeks. As illustrated in Figure 6A, the mean tumor volume in hispolon-treated mice was smaller compared to that of mice injected with only vehicle at 15 days. Weights of HL-60 xenografts were reduced by (29 ± 2.26)% and (34 ± 1.68)% after 15 days of treatment with 5 and 10 mg/kg hispolon, respectively (Figure 6B). No significant difference in body weight was detected among these groups (Figure 6C). To examine whether hispolon exerts antitumor activity in vivo via proliferation inhibition, proliferating cells were indicated by Ki67 immunocytochemical staining. Mean numbers of Ki67-positive tumor cells after treatment with 5 and 10 mg/kg hispolon were reduced (27.8 ± 4.26)% and (36.1 ± 3.85)%, respectively, compared to control mice (Figure 6D). We further detected procaspase protein levels of HL-60 xenografts harvested from vehicle- or hispolon-treated mice and found that levels of procaspase-3 were reduced in the tumors isolated from hispolon-treated mice (Figure 6E), suggesting that induction of cell apoptosis was involved in the hispolon-induced decrease in the tumor size. These results suggest that hispolon is effective against HL-60 cell growth in vivo.

DISCUSSION

The present study was undertaken to investigate the antitumor effect of hispolon on AML and its underlying mechanisms. Our in vitro studies demonstrated that hispolon inhibited cell proliferation in six human AML cell lines, THP-1, U937, HL-60, OCI, MV4-11, and MOLM-13. IC_{50} values of hispolon on these AML cell lines (6.25−25 μM) were lower than those for other solid tumor cells, such as breast and bladder cancer (IC_{50} 20−40 μM),[17] gastric cancer (IC_{50} 30 μM),[18] and liver cancer (IC_{50} 36−88 μM).[16] Our data suggest that these AML cell lines were more sensitive to hispolon-mediated inhibition of cell viability than several other types of solid tumor cells. In vivo studies showed that i.p. administration of hispolon at a dose of 5 or 10 mg/kg caused a substantial decline in the size of HL-60 tumor masses. A decreased number of Ki67-immunoreactive-positive cells in HL-60 xenografts isolated from hispolon-treated mice suggests that hispolon exerts an antitumor activity in vivo via inhibition of cancer cell proliferation. To the best of our knowledge, this is the first demonstration of the antitumor effect of hispolon on AML in vitro and in vivo.

Apoptosis, characterized by morphological changes such as membrane blebbing, cell shrinkage, chromatin condensation, and nuclear fragmentation with formation of apoptotic bodies, is a form of programmed cell death that occurs naturally in cells and can be beneficial to cancer therapy as previously reported.[27,28] Recently, targeted elimination of AML cells by inducing apoptosis has emerged as a valuable strategy for combating AML.[5,29] Moreover, several naturally occurring drugs such as homoharringtonine and etoposide are used in the clinic for treating AML.[30] In this study, several hallmarks of apoptosis such as significant increases in chromatin condensation, the sub-G_1 content, and Annexin V-positive cells were observed in HL-60 cells after hispolon treatment for 24 h. Fifty micromolar hispolon can induce increases of sub-G1 content and Annexin V-positive cells by 21.3- and 10.3-fold, respectively.

It is widely recognized that apoptosis is initiated by two principal pathways: a mitochondrion-mediated intrinsic pathway and a death-receptor-induced extrinsic pathway.[31] Caspases are believed to play crucial roles in mediating various apoptotic responses. A model involving two different caspases (caspase-8 and -9) in mediating distinct types of apoptotic stimuli was proposed. The cascade led by caspase-8 is involved in death receptor-mediated apoptosis, such as the one triggered by Fas. Ligation of Fas by the Fas ligand results in sequential recruitment of the Fas-associated death domain (FADD) and procaspase-8 to death domain of Fas to form a death-inducing signaling complex, leading to cleavage of procaspase-8, with consequent generation of active caspase-8.[32] Active caspase-8 in turn activates Bid and then triggers the mitochondrial pathway or directly activates caspase-3, committing the cell to apoptosis.[33] The present results suggest that hispolon may partially act through the initiator caspase-8 and then the executioner caspase-3 to increase the cleavage form of PARP to induce AML cell apoptosis. Moreover, many papers pointed out that the ability of anticancer agents to induce apoptosis of tumor cells was correlated with the ability to decrease expression of Bcl-2.[34] In our study, we found that expression of Bcl-2 decreased as the concentration of hispolon and percentage of apoptotic HL-60 cells increased. This inverse proportional relationship suggested that Bcl-2 may play a preventive role in hispolon-mediated apoptosis of HL-60 cells. Mitochondrion-dependent apoptosis is often controlled by Bcl-2 family members, which can be classified into three subfamilies: antiapoptotic members such as Bcl-2, Bcl-XL, and Mcl-1; proapoptotic members such as Bax and Bak; and BH3 (Bcl-2 homology domain 3)-only members such as Bim and Bad.[35] Bcl-2 is present in the outer mitochondrial membrane, where it functions to suppress apoptosis via blocking cytochrome *c* release and binding to Apaf-1. In the presence of excess Bax, Bcl-2 is displaced from Apaf-1, which further activates caspases-9/-3 and promotes apoptosis. In the present study, a decrease in the Bcl-2/Bax protein ratio, an increase in the collapse of mitochondrial membrane potential, and activation of caspases-9/-3 occurred in HL-60 cells after treatment with hispolon, suggesting that hispolon inducing apoptosis in HL-60 cells might partly occur through a mitochondrion-mediated pathway.

MAPKs are composed of several subfamilies, including ERK1/2, JNKs, and p38. These subfamilies regulate a variety of cellular responses, such as cell proliferation, differentiation, and apoptosis.[36,37] On the basis of previous reports that MAPKs are involved in the effects of hispolon in solid tumor cells,[16,17] we investigated activation of MAPK family proteins in hispolon-treated HL-60 cells. The results showed that JNK, ERK, and p38 were phosphorylated after hispolon treatment and 50 μM hispolon induced activation of JNK, ERK, and p38 by 8.3-, 11.5-, and 18.8-fold, respectively. However, only the JNK-specific inhibitor, SP600125, effectively reversed activation of caspases-8, -9, and -3 induced by hispolon, whereas SB202190 (a p38 inhibitor) and U0126 (an ERK inhibitor) had no effect on hispolon-induced caspase activation. Also, JNK-specific siRNA knockdown experiments showed that knockdown of JNK expression prevented hispolon-induced caspases activation.

JNK, an important mediator of apoptosis, was reported to regulate the function of Bcl-2 family proteins.[38,39] Previous reports indicated that JNK can phosphorylate Bcl-2, which modulates ubiquitin-mediated degradation of Bcl-2 and inhibits its antiapoptotic properties.[38,40] Surprisingly, pretreatment with SP600125 did not block downregulation of Bcl-2 induced by hispolon in our study (Figure 3, Supporting Information). Taken together, these results suggest that activation of JNK plays an important role in hispolon-induced apoptosis of HL-60 cells via regulation of caspase-8, -9, and -3 activities but not Bcl-2 expression. Bcl-2 is regulated by various mechanisms, including transcription, post-translational modifications, and degradation. Cyclic AMP response element is the major positive regulatory site in the *Bcl-2* promoter.[41] This element is required for binding of Nuclear Factor-KappaB (NF-κB) and cAMP-response element binding protein (CREB), which results in activation of Bcl-2 expression in lymphoma cells.[42,43] In AML, the effect of hispolon on the binding activity of NF-κB or CREB on *Bcl-2* promoter warrants further study in our future work. In addition to Bcl-2, JNK also phosphorylates BH3-only members of the Bcl-2 family such as Bim, which activates pro-apoptotic Bax and Bak and then induces mitochondrion-mediated caspases activation.[44] Moreover, it has also been reported that apoptosis induction by JNK activation involves Bim, and their pro-apoptotic potential was induced by reactive oxygen species (ROS). The role of ROS and Bim in hispolon-mediated caspases activation will be further investigated in our future work, too.

Moreover, we first examined the in vivo anticancer effect of hispolon in an NSG mouse tumor model. Hispolon effectively

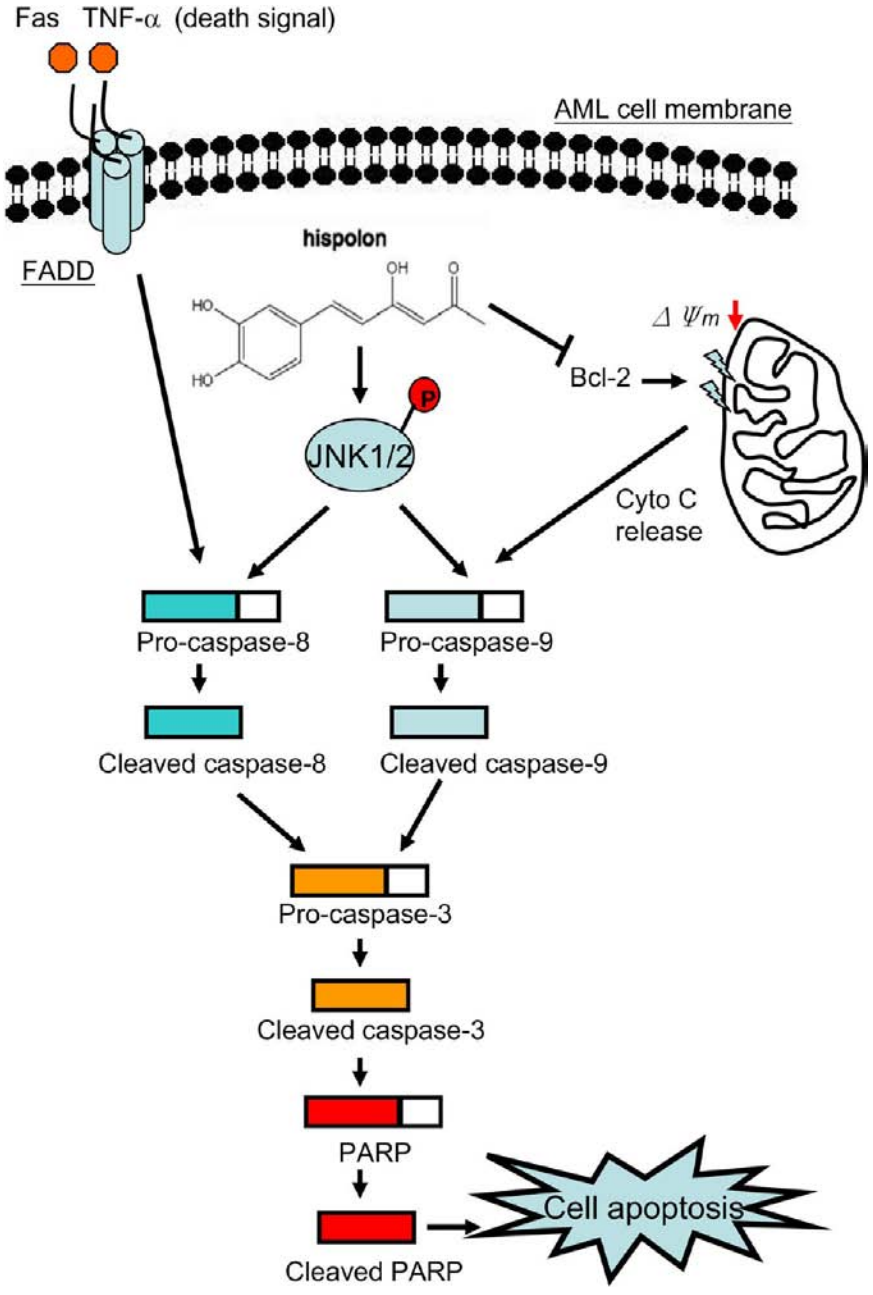

Figure 7. Proposed signal transduction pathways by which hispolon induces apoptosis of HL-60 cells. Anticancer activity of hispolon can be attributed to its apoptosis induction of AML cells via both the mitochondrial and the death receptor apoptosis pathways by suppressing Bcl-2 expression, inducing mitochondria membrane potential ($\Delta\Psi_m$) loss and inducing JNK1/2 and caspase-8, -9, and -3 activation.

attenuated tumor growth, even at a lower dose. In the hispolon-treated group, both the tumor volume and the weight were significantly reduced compared with those of the control group. These results further confirmed the anticancer effect of hispolon and its clinical potential.

In summary, the present study first demonstrated that hispolon possessed an antileukemic effect on AML cells in vitro and in vivo; the schematic mechanism is illustrated in Figure 7. The anticancer activity of hispolon can be attributed to its inhibition of proliferation and apoptosis induction of AML cells via both the mitochondrial and the death receptor apoptosis pathways by suppressing Bcl-2 expression, inducing mitochondria membrane potential loss, and inducing JNK1/2 and caspase-8, -9, and -3 activation. Our findings revealed that hispolon may be a useful candidate as a chemotherapeutic agent for AML therapy.

■ ASSOCIATED CONTENT

Supporting Information

Effect of hispolon on the cell viability of human normal cells; effect of hispolon on the JNK activation; effect of JNK specific inhibitor on hispolon-mediated suppression of Bcl-2. This material is available free of charge via the Internet at http://pubs.acs.org.

■ AUTHOR INFORMATION

Corresponding Author

*E-mail: mhchien1976@gmail.com.

Author Contributions

Pei-Ching Hsiao and Yi-Hsien Hsieh contributed equally to this work.

Funding

This study was supported by a grant (no. 102 swf03) from Wan Fang Hospital-Taipei Medical University and by a grant (CSH-2013-C-001) from Chung Shan Medical University Hospital, Taiwan.

Notes

The authors declare that there is no conflict of interest. The authors declare no competing financial interest.

■ ABBREVIATIONS USED

AML, acute myeloid leukemia; PI, propidium iodide; DAPI, 4′,6-diamidino-2-phenylindole; PARP, poly-ADPribose polymerase; JNK, c-Jun N-terminal kinase; ERK, extracellularly regulated kinase; siRNA, small interfering RNA; PL, *Phellinus linteus*; NSG, NOD/SCID-IL2Rγ^{null}

■ REFERENCES

(1) Bishop, J. F. The treatment of adult acute myeloid leukemia. *Semin. Oncol.* **1997**, *24* (1), 57−69.

(2) Tallman, M. S.; Gilliland, D. G.; Rowe, J. M. Drug therapy for acute myeloid leukemia. *Blood* **2005**, *106* (4), 1154−1163.

(3) Huang, S. T.; Wang, C. Y.; Yang, R. C.; Chu, C. J.; Wu, H. T.; Pang, J. H. Wogonin, an active compound in scutellaria baicalensis, induces apoptosis and reduces telomerase activity in the hl-60 leukemia cells. *Phytomedicine* **2010**, *17* (1), 47−54.

(4) Kang, S. H.; Jeong, S. J.; Kim, S. H.; Kim, J. H.; Jung, J. H.; Koh, W.; Kim, D. K.; Chen, C. Y. Icariside ii induces apoptosis in u937 acute myeloid leukemia cells: Role of inactivation of stat3-related signaling. *PLoS One* **2012**, *7* (4), e28706.

(5) Zhang, S.; Zhang, Y.; Zhuang, Y.; Wang, J.; Ye, J.; Wu, J.; Yu, K.; Han, Y. Matrine induces apoptosis in human acute myeloid leukemia cells via the mitochondrial pathway and akt inactivation. *PLoS One* **2012**, *7* (10), e46853.

(6) Park, H. G.; Shim, Y. Y.; Choi, S. O.; Park, W. M. New method development for nanoparticle extraction of water-soluble beta-(1−>3)-d-glucan from edible mushrooms, sparassis crispa and phellinus linteus. *J. Agric. Food Chem.* **2009**, *57* (6), 2147−2154.

(7) Guo, J.; Zhu, T.; Collins, L.; Xiao, Z. X.; Kim, S. H.; Chen, C. Y. Modulation of lung cancer growth arrest and apoptosis by phellinus linteus. *Mol. Carcinog.* **2007**, *46* (2), 144−154.

(8) Zhu, T.; Guo, J.; Collins, L.; Kelly, J.; Xiao, Z. J.; Kim, S. H.; Chen, C. Y. Phellinus linteus activates different pathways to induce apoptosis in prostate cancer cells. *Br. J. Cancer* **2007**, *96* (4), 583−590.

(9) Lee, H. J.; Lim, E. S.; Ahn, K. S.; Shim, B. S.; Kim, H. M.; Gong, S. J.; Kim, D. K.; Kim, S. H. Cambodian phellinus linteus inhibits experimental metastasis of melanoma cells in mice via regulation of urokinase type plasminogen activator. *Biol. Pharm. Bull.* **2005**, *28* (1), 27−31.

(10) Jeon, T.; Hwang, S. G.; Jung, Y. H.; Yang, H. S.; Sung, N. Y.; Lee, J.; Park, D. K.; Yoo, Y. C. Inhibitory effect of oral administration of sangwhang mushroom (Phellinus linteus) grown on germinated brown rice on experimental lung metastasis and tumor growth in mice. *Food Sci. Biotechnol.* **2011**, *20* (1), 209−214.

(11) Sliva, D.; Jedinak, A.; Kawasaki, J.; Harvey, K.; Slivova, V. Phellinus linteus suppresses growth, angiogenesis and invasive behaviour of breast cancer cells through the inhibition of akt signalling. *Br. J. Cancer* **2008**, *98* (8), 1348−1356.

(12) Ali, N. A.; Ludtke, J.; Pilgrim, H.; Lindequist, U. Inhibition of chemiluminescence response of human mononuclear cells and suppression of mitogen-induced proliferation of spleen lymphocytes of mice by hispolon and hispidin. *Pharmazie* **1996**, *51* (9), 667−670.

(13) Venkateswarlu, S.; Ramachandra, M. S.; Sethuramu, K.; Subbaraju, G. V. Synthesis and antioxidant activity of hispolon, a yellow pigment from Inonotus hispidius. *Indian J. Chem. B* **2002**, *41* (4), 875−877.

(14) Huang, G. J.; Deng, J. S.; Chiu, C. S.; Liao, J. C.; Hsieh, W. T.; Sheu, M. J.; Wu, C. H. Hispolon protects against acute liver damage in the rat by inhibiting lipid peroxidation, proinflammatory cytokine, and oxidative stress and downregulating the expressions of inos, cox-2, and mmp-9. *J. Evidence-Based Complementary Altern. Med.* **2012**, *2012*, 480714.

(15) Chien, Y. C.; Huang, G. J.; Cheng, H. C.; Wu, C. H.; Sheu, M. J. Hispolon attenuates balloon-injured neointimal formation and modulates vascular smooth muscle cell migration via akt and erk phosphorylation. *J. Nat. Prod.* **2012**, *75* (9), 1524−1533.

(16) Huang, G. J.; Deng, J. S.; Huang, S. S.; Hu, M. L. Hispolon induces apoptosis and cell cycle arrest of human hepatocellular carcinoma hep3b cells by modulating erk phosphorylation. *J. Agric. Food Chem.* **2011**, *59* (13), 7104−7113.

(17) Lu, T. L.; Huang, G. J.; Lu, T. J.; Wu, J. B.; Wu, C. H.; Yang, T. C.; Iizuka, A.; Chen, Y. F. Hispolon from phellinus linteus has antiproliferative effects via mdm2-recruited erk1/2 activity in breast and bladder cancer cells. *Food Chem. Toxicol.* **2009**, *47* (8), 2013−2021.

(18) Chen, W.; Zhao, Z.; Li, L.; Wu, B.; Chen, S. F.; Zhou, H.; Wang, Y.; Li, Y. Q. Hispolon induces apoptosis in human gastric cancer cells through a ros-mediated mitochondrial pathway. *Free Radical Biol. Med.* **2008**, *45* (1), 60−72.

(19) Chen, W.; He, F. Y.; Li, Y. Q. The apoptosis effect of hispolon from phellinus linteus (berkeley & curtis) teng on human epidermoid kb cells. *J. Ethnopharmacol.* **2006**, *105* (1−2), 280−285.

(20) Huang, G. J.; Yang, C. M.; Chang, Y. S.; Amagaya, S.; Wang, H. C.; Hou, W. C.; Huang, S. S.; Hu, M. L. Hispolon suppresses sk-hep1 human hepatoma cell metastasis by inhibiting matrix metalloproteinase-2/9 and urokinase-plasminogen activator through the pi3k/akt and erk signaling pathways. *J. Agric. Food Chem.* **2010a**, *58* (17), 9468−9475.

(21) Hwang, J. M.; Kao, S. H.; Hsieh, Y. H.; Li, K. L.; Wang, P. H.; Hsu, L. S.; Liu, J. Y. Reduction of anion exchanger 2 expression induces apoptosis of human hepatocellular carcinoma cells. *Mol. Cell. Biochem.* **2009**, *327* (1−2), 135−144.

(22) Chen, M. W.; Hua, K. T.; Kao, H. J.; Chi, C. C.; Wei, L. H.; Johansson, G.; Shiah, S. G.; Chen, P. S.; Jeng, Y. M.; Cheng, T. Y.; Lai, T. C.; Chang, J. S.; Jan, Y. H.; Chien, M. H.; Yang, C. J.; Huang, M. S.; Hsiao, M.; Kuo, M. L. H3k9 histone methyltransferase g9a promotes lung cancer invasion and metastasis by silencing the cell adhesion molecule ep-cam. *Cancer Res.* **2010**, *70* (20), 7830−7840.

(23) Chien, M. H.; Lee, T. S.; Kao, C.; Yang, S. F.; Lee, W. S. Terbinafine inhibits oral squamous cell carcinoma growth through anti-cancer cell proliferation and anti-angiogenesis. *Mol. Carcinog.* **2012**, *51* (5), 389−399.

(24) Khan, N.; Afaq, F.; Mukhtar, H. Apoptosis by dietary factors: The suicide solution for delaying cancer growth. *Carcinogenesis* **2007**, *28* (2), 233−239.

(25) Kim, R.; Emi, M.; Tanabe, K. Role of mitochondria as the gardens of cell death. *Cancer Chemother. Pharmacol.* **2006**, *57* (5), 545−553.

(26) Chen, T.; Wong, Y. S. Selenocystine induces s-phase arrest and apoptosis in human breast adenocarcinoma mcf-7 cells by modulating erk and akt phosphorylation. *J. Agric. Food Chem.* **2008**, *56* (22), 10574−10581.

(27) Chinkwo, K. A. Sutherlandia frutescens extracts can induce apoptosis in cultured carcinoma cells. *J. Ethnopharmacol.* **2005**, *98* (1−2), 163−170.

(28) Kroemer, G.; Martin, S. J. Caspase-independent cell death. *Nat. Med.* **2005**, *11* (7), 725−730.

(29) Carter, B. Z.; Mak, D. H.; Shi, Y.; Fidler, J. M.; Chen, R.; Ling, X.; Ling, X.; Plunkett, W.; Andreeff, M. Mrx102, a triptolide derivative, has potent antileukemic activity in vitro and in a murine model of aml. *Leukemia* **2012**, *26* (3), 443−450.

(30) Efferth, T.; Li, P. C.; Konkimalla, V. S.; Kaina, B. From traditional chinese medicine to rational cancer therapy. *Trends Mol. Med.* **2007**, *13* (8), 353−361.
(31) Spencer, S. L.; Sorger, P. K. Measuring and modeling apoptosis in single cells. *Cell* **2011**, *144* (6), 926−939.
(32) Thorburn, A. Death receptor-induced cell killing. *Cell. Signalling* **2004**, *16* (2), 139−144.
(33) Yin, X. M. Bid, a critical mediator for apoptosis induced by the activation of fas/tnf-r1 death receptors in hepatocytes. *J. Mol. Med. (Berlin)* **2000**, *78* (4), 203−211.
(34) Vermes, I.; Haanen, C.; Steffens-Nakken, H.; Reutelingsperger, C. A novel assay for apoptosis. Flow cytometric detection of phosphatidylserine expression on early apoptotic cells using fluorescein labelled annexin v. *J. Immunol. Methods* **1995**, *184* (1), 39−51.
(35) Cotter, T. G. Apoptosis and cancer: The genesis of a research field. *Nat. Rev. Cancer* **2009**, *9* (7), 501−507.
(36) Matsukawa, J.; Matsuzawa, A.; Takeda, K.; Ichijo, H. The ask1-map kinase cascades in mammalian stress response. *J. Biochem.* **2004**, *136* (3), 261−265.
(37) Cobb, M. H. Map kinase pathways. Prog. Biophys. *Mol. Biol.* **1999**, *71* (3−4), 479−500.
(38) Deng, X.; Xiao, L.; Lang, W.; Gao, F.; Ruvolo, P.; May, W. S., Jr. Novel role for jnk as a stress-activated bcl2 kinase. *J. Biol. Chem.* **2001**, *276* (26), 23681−23688.
(39) Fan, M.; Goodwin, M.; Vu, T.; Brantley-Finley, C.; Gaarde, W. A.; Chambers, T. C. Vinblastine-induced phosphorylation of bcl-2 and bcl-xl is mediated by jnk and occurs in parallel with inactivation of the raf-1/mek/erk cascade. *J. Biol. Chem.* **2000**, *275* (39), 29980−29985.
(40) Breitschopf, K.; Haendeler, J.; Malchow, P.; Zeiher, A. M.; Dimmeler, S. Posttranslational modification of bcl-2 facilitates its proteasome-dependent degradation: Molecular characterization of the involved signaling pathway. *Mol. Cell. Biol.* **2000**, *20* (5), 1886−1896.
(41) Wilson, B. E.; Mochon, E.; Boxer, L. M. Induction of bcl-2 expression by phosphorylated CREB proteins during B-cell activation and rescue from apoptosis. *Mol. Cell. Biol.* **1996**, *16* (10), 5546−5556.
(42) Heckman, C. A.; Mehew, J. W.; Boxer, L. M. NF-kappaB activates Bcl-2 expression in t(14;18) lymphoma cells. *Oncogene* **2002**, *21* (24), 3898−3908.
(43) Xiang, H.; Wang, J.; Boxer, L. M. Role of the cyclic AMP response element in the bcl-2 promoter in the regulation of endogenous Bcl-2 expression and apoptosis in murine B cells. *Mol. Cell. Biol.* **2006**, *26* (22), 8599−8606.
(44) Szegezdi, E.; Logue, S. E.; Gorman, A. M.; Samali, A. Mediators of endoplasmic reticulum stress-induced apoptosis. *EMBO Rep* **2006**, *7* (9), 880−885.
(45) Chinen, T.; Nagumo, Y.; Watanabe, T.; Imaizumi, T.; Shibuya, M.; Kataoka, T.; Kanoh, N.; Iwabuchi, Y.; Usui, T. Irciniastatin A induces JNK activation that is involved in caspase-8-dependent apoptosis via the mitochondrial pathway. *Toxicol. Lett.* **2010**, *199* (3), 341−346.